SOLAR THERMOPHOTOVOLTAIC ENERGY CONVERSION SYSTEMS WITH TANTALUM PHOTONIC CRYSTAL ABSORBERS AND EMITTERS

Youngsuk Nam[1,2], Andrej Lenert[1], Yi Xiang Yeng[1], Peter Bermel[1], Marin Soljačić[1] and Evelyn N. Wang[1]*
[1]Massachusetts Institute of Technology, Cambridge, USA
[2] Kyung Hee University, Yongin, Korea

ABSTRACT

We investigated the performance of solar thermophotovoltaic (STPV) systems with 2D tantalum (Ta) PhCs using thermophotovoltaic experiments and a high-fidelity thermal electrical system-level model. The experimental data obtained with 1D PhCs matched the predicted results within experimental uncertainty. The model predicts that the absorber-to-electrical efficiency of a planar STPV consisting of an optimized 2D Ta PhC absorber/emitter and current state of the art InGaAsSb PV cell with a tandem filter can be as high as ~10% at an irradiation flux of ~130 kW/m^2. This work offers a framework and guidelines to improve the performance of both PhCs and overall STPV systems.

KEYWORDS

Thermophotovoltaic, solar, photonic crystal, tantalum, STPV, TPV, emitter, absorber.

INTRODUCTION

Solar thermophotovoltaic (STPV) systems use an intermediate module that absorbs the solar radiation, and re-radiates photons at high temperatures with tailored wavelengths toward a photovoltaic (PV) cell (Fig.1). By converting the incident solar radiation to a narrow-band thermal emission matched to the spectral response of the PV cell, STPVs have the potential to overcome the Shockley-Queisser limit for the efficiency of PVs (~33% for 1 sun) [1, 2]. STPVs are also highly scalable for a wide range of power capacities, have no moving parts, and allow solar energy storage and the use of an alternative fuel to generate electricity.

Despite the significant potential of STPVs, very few experimental results have reported the system-level efficiency of these systems. Meanwhile, of those reported, the overall efficiencies were relatively low (~1%) due to the poor performance of the emitter, absorber, and PV cell and insufficient understanding of the highly coupled energy transport processes among these components [3, 4]. Recently, the use of photonic crystals (PhCs) with 1D periodic metal/dielectric layers, 2D arrays of cavities and 3D woodpile structures have been suggested to overcome this challenge [5-10]. These previous studies with PhCs, however, have focused on component level rather than system level performance. Therefore the realistic performance of STPVs and the energy loss mechanisms associated with the integration of these components have not been fully investigated.

In this work, we report the performance analysis of planar STPVs with 2D Ta PhCs absorbers and emitters. We optimized the 2D Ta PhC design and developed a high-fidelity axisymmetric thermal-electrical hybrid system-level model for STPVs. TPV experiments were also conducted by varying the emitter temperature with two different PV cells to validate the model.

SYSTEM-LEVEL STPV MODEL

The simplified schematic of a planar STPV is shown in Figure 1. Due to the multiple energy conversion and transport steps in STPVs, the overall efficiency is determined from the balance between various component-level efficiencies:

$$\eta_{overall} = \frac{H_{abs}\cdot A_{abs}}{H_c \cdot A_c}\cdot\frac{Q_{abs}}{H_{abs}\cdot A_{abs}}\cdot\frac{|Q_{emit}|}{Q_{abs}}\cdot\frac{|Q_{emit,(E\geq E_g)}|}{|Q_{emit}|}\cdot\frac{Q_{cell,(E\geq E_g)}}{|Q_{emit,(E\geq E_g)}|}\cdot\frac{P_{elec,\max}}{Q_{cell,(E\geq E_g)}}$$
$$= \eta_{collector}\cdot\eta_{absorber}\cdot\eta_{adiabatic}\cdot\eta_{spectral}\cdot\eta_{cavity}\cdot\eta_{cell} \quad , \quad (1)$$
$$= \eta_{collector}\cdot\eta_{STPV(abs-elec)}$$

where H_c and H_{abs} represent the amount of solar irradiation flux incident onto the collector and absorber surfaces, respectively. The A_c and A_{abs} are the areas of the collector and absorber. Q_{abs}, Q_{emit} and Q_{cell} represent the net amount of heat applied to the absorber, emitter and PV cell surfaces, respectively. $P_{elec,max}$ is the maximum power output produced by the PV cell whose band gap is E_g.

We define the absorber- to-electrical STPV efficiency $\eta_{STPV(abs-elec)}$ that excludes the collector loss from the overall efficiency as in Eq.1 to focus on the effects of the PhC emitters and absorbers on the STPV performance.

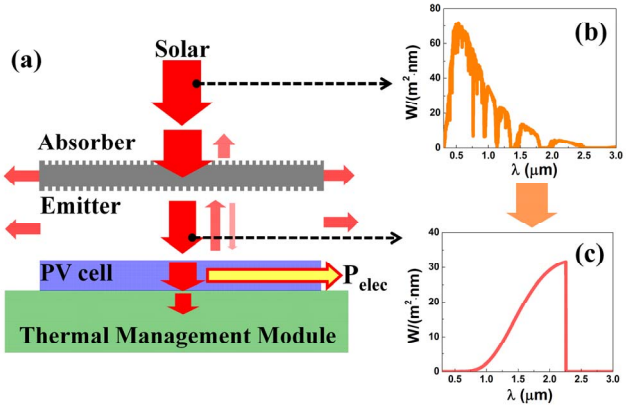

Figure 1: (a) Schematic of a planar STPV that converts solar radiation with a wide spectrum (b) into a tailored spectrum matched to the spectral response of the PV cell (c).

We developed a steady-state thermal-electrical hybrid system-level STPV model using the finite element method and an equivalent circuit model. The radiative heat

transfer is coupled with conductive and convective heat transfer on each infinitesimal boundary element defined in a 2D axisymmetric framework. For a realistic prediction, various optical and electrical cell performance parameters are determined based on previous experimental characterization [11, 12].

EXPERIMENTAL VALIDATION

Experimental system

We designed the experimental system for characterizing high-temperature planar STPVs aiming to validate the developed model. The following experimental capabilities were developed to properly account for the coupled energy conversion steps and to measure the STPV device characteristics: incident power of simulated solar radiation, absorber/emitter temperature, current-voltage (IV) characterization, and thermal load on the PV cell. The experimental layout (Fig.2a) minimizes parasitic heat losses while allowing for precise alignment and gap control between the absorber-emitter and the PV cell. An accurate measurement of the emitter temperature with minimal impact on the temperature distribution of the emitter was obtained using a thin gauge thermocouple bonded to the back of the emitter substrate (Fig.2b).

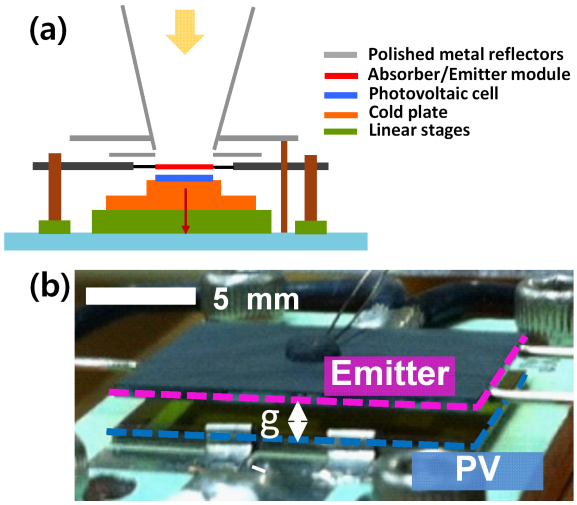

Figure 2: (a) Schematic of the STPV experimental layout used to achieve precise alignment and spacing between the emitter and PV, and temperature control of the PV. (b) Image of the TPV device showing the gap between with emitter and PV, and placement of the bonded thermocouple.

Using the experimental system, we investigated a solar-powered TPV system composed of a one-dimensional photonic crystal (1D PhC) as a high-temperature spectrally selective emitter paired with two different photovoltaic (PV) cells: GaSb (0.72 eV) and InGaAsSb (0.55 eV). The multilayer Si/SiO_2 structure of the 1D PhC improves the spectral matching between the emissivity of the emitter and the quantum efficiency of the PVs (Fig.3); particularly with the lower bandgap InGaAsSb PV.

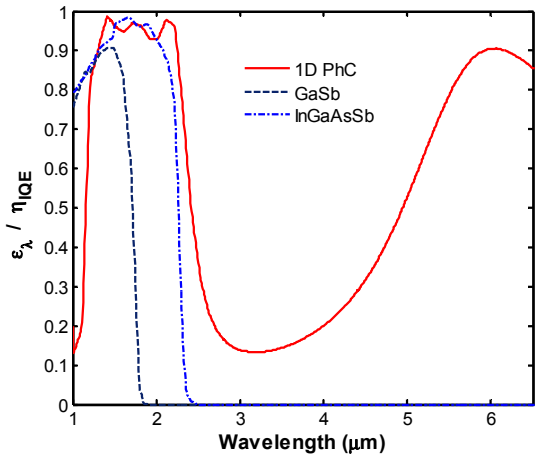

Figure 3: Spectral emissivity of the 1D Si/SiO_2 PhC (measured at 1293K) compared to the internal quantum efficiency (IQE) of the GaSb and InGaAsSb PVs.

IV characteristics

The IV characteristics of the TPV were experimentally characterized by controlling the solar power incident on the device, and accordingly varying the emitter temperature from room temperature to above 1200 K. The maximum power generated by the PVs was measured from the IV sweep as a function of the 1D PhC emitter temperature. As shown in Figure 4, the power generated by the 1D PhC/InGaAsSb TPV greatly exceeds its 1D PhC/GaSb TPV counterpart, primarily due to the improved spectral matching between the emitter and the PV.

Predictions using a detailed numerical model match the results within experimental uncertainty, validating the numerical models used throughout this study. The demonstrated TPV (thermal-to-electrical) efficiency of the 1D PhC/InGaAsSb TPV (5.1 % at 1275 K) are significantly higher than for the 1D PhC/GaSb TPV (1.7 % at 1225 K). These efficiencies represent more than a two-fold improvement over blackbody-based emitter TPV systems without any spectral control.

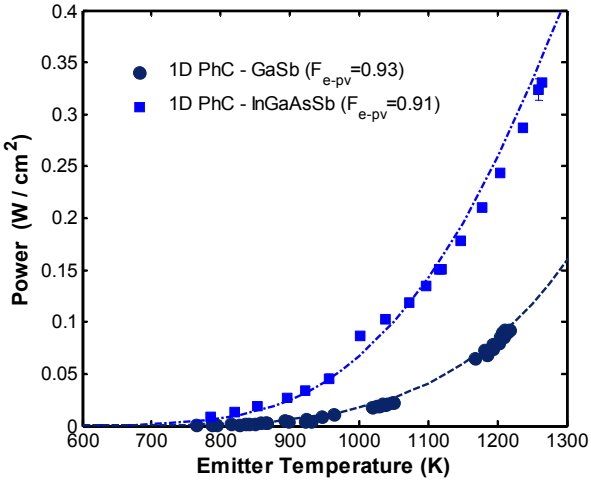

Figure 4: Maximum power output as a function of emitter temperature for two TPV cases: a 1D Si/SiO_2 PhC emitter paired with GaSb (JX crystal) PV and with a InGaAsSb PV. The view factor ($F_{e\text{-}pv}$) between the emitter and PV in both cases exceeds 0.9. Line and symbols represent the results obtained from the model and experiments, respectively.

Nonetheless, the overall energy conversion efficiency is limited by non-idealities of the emitter/PVs and imperfect spectral matching between the emitter emissivity and quantum efficiency such as the high emissivity peak of the 1D PhC centered around 6 μm. Accordingly, these results motivate STPV designs with spectrally engineered 2D PhCs for improved overall system-level performance.

MODEL RESULTS

Optimized 2D Tantalum photonic crystals

In order to further enhance the spectral performance of the absorber and emitter, we engineered the radiative spectra of emitters and absorbers using a two-dimensional square array of cylindrical holes with period (p), diameter (d), and depth (h) created on a tantalum (Ta) substrate (see the inset of Fig. 5). Ta was selected due to its high melting point (3290 K), low vapor pressure and good intrinsic spectral selectivity. The 2D Ta PhC absorber and emitter exhibit near-blackbody emittance at short wavelengths as well as emittance almost as low as a polished metal at long wavelengths, with a sharp cutoff separating the two regimes. The cutoff wavelength is tunable by adjusting the fundamental cavity resonant frequency through changes in the dimensions of the cavities, while the maximum emittance of the first resonance peak below the cutoff is achieved via Q-matching [7]

The optimization was performed using a figure of merit (FOM) measuring how close the performance is compared to an ideal cutoff emitter:

$$FOM = 0.75\overline{E}_{\lambda \le \lambda_{cut}} + 0.25(1 - \overline{E}_{\lambda > \lambda_{cut}}) \quad , \quad (2)$$

where $\overline{E}_{\lambda \le \lambda_{cut}}$ and $\overline{E}_{\lambda > \lambda_{cut}}$ represent the average emittance above and below the band gap, respectively. Figure 5 shows the resulting optimized radiative spectra of 2D Ta PhCs and flat Ta obtained at 1200 K. Both normal (N) and hemispherically averaged (H) emittance are provided.

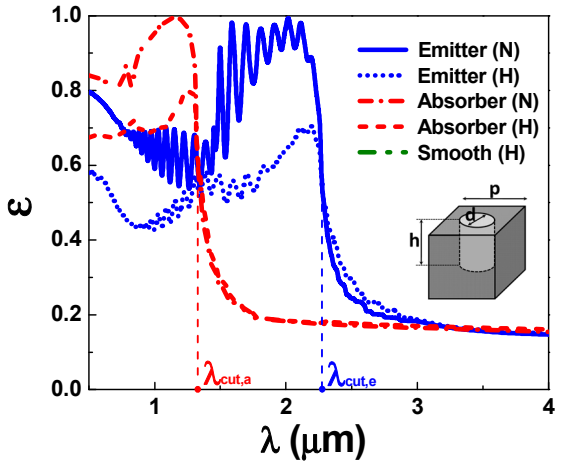

Figure 5: Normal (N) and hemispherically averaged (H) emittance at T=1200 K for the developed 2D Ta PhC absorber/emitter and smooth Ta. The optimal cavity dimensions are determined to be p = 0.68 μm, d = 0.78 μm, h = 7.94 μm for the absorber, and p = 1.24 μm, d = 1.45 μm, h = 8.00 μm for the emitte, respectively.

Efficiency of STPVs with 2D Ta PhCs

The optimized 2D Ta PhCs were incorporated into the system-level STPV model. To focus on the effect of the PhCs, a simple planar layout composed of a co-axial circular absorber/emitter/PV cell of the same size is investigated. Collimated and uniform incident solar radiation is applied to the absorber. Convective losses and conduction between the emitter and PV cell are neglected by considering a vacuum environment. A list of the considered STPV configurations is provided in Table 1.

Table 1: Simulated STPV configurations. Normalized thickness(t/R) and gap(g/R) are fixed at 0.05 for all cases.

	Absorber	Emitter	Cell front	PV cell
Case I	Ideal cutoff	Ideal cutoff	Black body	Ideal [13] (0.55 eV)
Case II	Ta PhC (Fig.5)	Ta PhC (Fig.5)	Black body	Ideal (0.55 eV)
Case III	Ta PhC (Fig.5)	Ta PhC (Fig.5)	AR coating	InGaAsSb (0.55eV) [12]
Case IV	Ta PhC (Fig.5)	Ta PhC (Fig.5)	Tandem filter [14]	InGaAsSb (0.55eV) [12]

Figure 6a and 6b show the system (absorber-to-electrical) and component-level efficiencies of SPTVs with the ideal cutoff (*Case I*) and 2D Ta PhC (*Case II*) absorber/emitter, respectively. Compared with the ideal cutoff emitter, the 2D Ta PhC emitter reduces the spectral efficiency η_{spec} over 40% due to the increase in low energy emission beyond $\lambda_{cut,e}$ and decrease in useful emission through the emittance offset below $\lambda_{cut,e}$. (Fig.6b). The increase in an irradiation flux onto the absorber (H_{abs}) enhances the spectral efficiency since the increase in emitter temperature reduces the relative portion of the low energy emission.

The 2D Ta PhC absorber also decreases the absorber efficiency η_{abs} over 35% compared with the ideal cutoff absorber due to the increase in the re-emission loss through the emittance offset beyond $\lambda_{cut,a}$. Therefore, the absorber-to-electrical efficiency decreases over 60% when the 2D Ta PhCs replace the ideal cutoff absorber/emitter. The optimal irradiation flux also shifts to a higher level to enhance the operating temperature and reduce the effects of non-ideal emittance offset beyond $\lambda_{cut,e}$.

Compared with the ideal PV cell (*Case II*), the implementation of the existing InGaAsSb PV cells drops the cell efficiency η_{cell} over 40% (*Case III*) due to the optical and electrical non-idealities in the cells. As a result, the absorber-to-electrical efficiency of the STPV composed of the optimized 2D Ta PhCs and the existing InGaAsSb PV cell is predicted to be approximately 8% at an irradiation flux of ~130 kW/m^2 and emitter temperature ~1350 K. Both adiabatic and cavity efficiencies were maintained around 95% in all cases and not plotted.

When the long wavelength reflection filter [14] is applied to the cell front surface (*Case IV*), the spectral efficiency increases over 30% but the absorber efficiency decreases by ~10% since the operating temperature increases by ~5% (Fig.6c). Accordingly, the overall efficiency increases by 15~20%, up to approximately 10% at an irradiation flux of ~130 kW/m^2 and emitter temperature ~1400 K (Fig.6a).

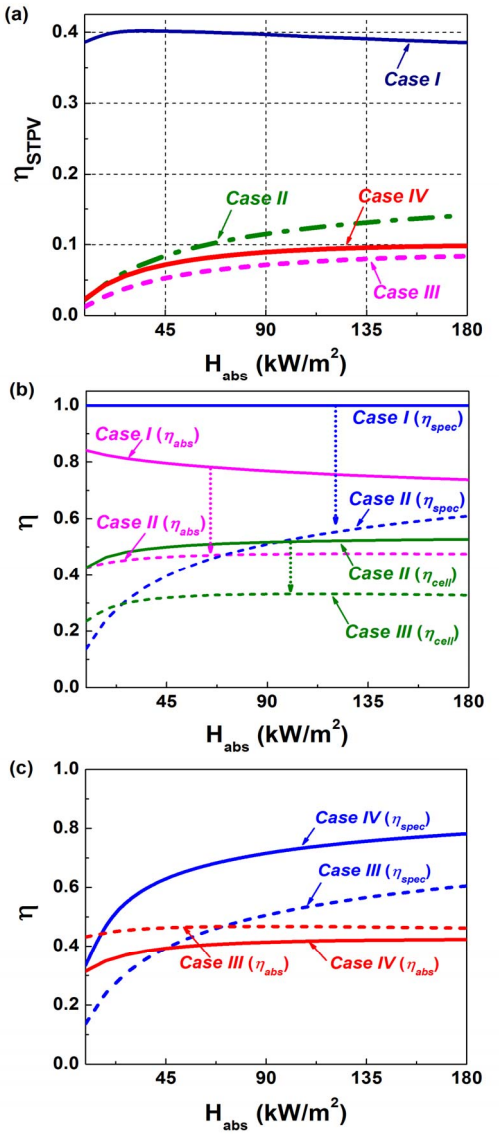

Figure 6: (a) Overall efficiencies of STPVs listed in Table 1 (Cases I-IV) and (b-c) Component level efficiencies of STPVs without (Case I-III) and with (Case IV) a tandem front filter.

CONCLUSION

We present the analysis of a planar STPV composed of 2D Ta PhCs and an existing PV cell/filter using TPV experiments and a high-fidelity thermal-electrical hybrid system-level STPV model. The experimental setup minimizing parasitic heat losses and allowing precise alignment was developed and the measured IV characteristics matched the predicted data well. By incorporating the optimized 2D Ta PhCs and current state of the art InGaAsSb PV cell with a tandem filter into our model, we show that the absorber-to-electrical STPV efficiency can be as high as ~10% with a simple planar layout (1:1 emitter-to-absorber area ratio) and a relatively low irradiation flux (~130 kW/m^2). The efficiency can be improved up to ~16% by eliminating the optical and electrical non-idealities in the PV cell.

ACKNOWLEDGEMENTS

This material is based upon work supported as part of the MIT S3TEC Center, an Energy Frontier Research Center funded by the U.S. Department of Energy, Office of Science, Office of Basic Energy Sciences under DE-FG02-09ER46577. Y.N. also acknowledges the support from Basic Science Research Program through the National Research Foundation of Korea (NRF) funded by the Ministry of Education, Science and Technology (No. 2012R1A1A1014845).

REFERENCE

[1] N.-P. Harder and P. Würfel, "Theoretical limits of thermophotovoltaic solar energy conversion," *Semiconductor Science and Technology,* vol. 18, p. S151, 2003.

[2] W. Shockley and H. J. Queisser, "Detailed Balance Limit of Efficiency of p-n Junction Solar Cells," *Journal of Applied Physics,* vol. 32, pp. 510-519, 1961.

[3] V. Khvostikov, *et al.*, "Thermophotovoltaic generators based on gallium antimonide," *Semiconductors,* vol. 44, pp. 255-262, 2010.

[4] H. Yugami, *et al.*, "Solar thermophotovoltaic using $Al_2O_3/Er_3Al_5O_{12}$ eutectic composite selective emitter," in *Photovoltaic Specialists Conference, 2000. Conference Record of the Twenty-Eighth IEEE*, 2000, pp. 1214-1217.

[5] P. Bermel, *et al.*, "Design and global optimization of high-efficiency thermophotovoltaic systems," *Opt. Express,* vol. 18, pp. A314-A334, 2010.

[6] I. Celanovic, *et al.*, "Two-dimensional tungsten photonic crystals as selective thermal emitters," *Applied Physics Letters,* vol. 92, pp. 193101-3, 2008.

[7] M. Ghebrebrhan, *et al.*, "Tailoring thermal emission via Q matching of photonic crystal resonances," *Physical Review A,* vol. 83, p. 033810, 2011.

[8] V. Mizeikis, *et al.*, "Three-dimensional woodpile photonic crystal templates forthe infrared spectral range," *Opt. Lett.,* vol. 29, pp. 2061-2063, 2004.

[9] M. U. Pralle, *et al.*, "Photonic crystal enhanced narrow-band infrared emitters," *Applied Physics Letters,* vol. 81, pp. 4685-4687, 2002.

[10] S. N. Veronika Rinnerbauer, *et al.*, "Recent developments in high-temperature photonic crystals for energy conversion," *Energy & Environmental Science,* vol. 5, pp. 8815-8823, 2012.

[11] W. Chan, *et al.*, "Modeling low-bandgap thermophotovoltaic diodes for high-efficiency portable power generators," *Solar Energy Materials and Solar Cells,* vol. 94, pp. 509-514, 2010.

[12] W. D. Michael, *et al.*, "Quaternary InGaAsSb Thermophotovoltaic Diodes," *Electron Devices, IEEE Transactions on,* vol. 53, pp. 2879-2891, 2006.

[13] P. Baruch, *et al.*, "On some thermodynamic aspects of photovoltaic solar energy conversion," *Solar Energy Materials and Solar Cells,* vol. 36, pp. 201-222, 1995.

[14] E. Brown, *et al.*, "The Status of Thermophotovoltaic Energy Conversion Technology at Lockheed Martin Corporation," LM-04K068, 2004.

CONTACT

*Evelyn N. Wang, +1 (617) 324-3311, enwang@mit.edu